EXPERIMENTAL MODEL TO ESTIMATE SHADING LOSSES ON PV ARRAYS.

F. Martínez-Moreno, J. Muñoz, E. Lorenzo

Instituto de Energía Solar - Universidad Politécnica de Madrid (IES-UPM).

E.T.S.I Telecomunicación. Ciudad Universitaria s/n. 28040 Madrid (Spain).

Correspondence to:

Francisco Martínez Moreno

Address: Instituto de Energía Solar – Universidad Politécnica de Madrid (IES-UPM).

E.T.S.I. Telecomunicación. Ciudad Universitaria s/n. 28040 Madrid (Spain).

E-mail: francisco.martinez@ies-def.upm.es

SUMMARY

This paper presents a simple mathematical model to estimate shading losses on PV arrays. The model is applied directly to power calculations, without the need to consider the whole current-voltage curve. This allows the model to be used with common yield estimation software. The model takes into account both the shaded fraction of the array area and the number of blocks (a group of solar cells protected by a bypass diode) affected by shade. The results of an experimental testing campaign on several shaded PV arrays to check the validity of model are also reported.

Keywords: power losses; shading model; PV array.

1. INTRODUCTION.

Photovoltaic (PV) plants are affected by shadows projected between PV arrays at sunrise and sunset. Obviously, shade is a normal situation which must be considered to achieve more accurate energy yield forecasts. Literature on the impact of shade on PV array output power is plentiful, with studies based on the consideration of the whole current-voltage (I-V) curve[ref]. This approach allows very accurate calculation with the careful consideration of all the details concerning interconnection between solar cells and bypass diodes. However, this also entails significant complexity (dealing with whole I-V curves means using non-linear equations[ref]) and computing time consumption (a well-defined I-V curve typically needs a minimum of 50 points[ref]). So, these models can hardly be considered for application in common energy yield estimation software[ref] which more often relies on direct power calculations. For this purpose a widely model used is[ref]:

$$P = P^* \cdot \frac{G}{G^*} \cdot \left[1 + \gamma \cdot \left(T_C - T_C^*\right)\right] \tag{1}$$

where P is the maximum array output power without shadow, G is the incident irradiance, T_C is the solar cell temperature, and γ is the power temperature coefficient. The superscript * stands for Standard Test Conditions (STC).

There is experimental evidence that, despite its great simplicity, equation (1) provides good accuracy[ref]. So, it is interesting to keep it, after proper modification, even when shadows appear on PV arrays.

2. THE PROPOSED MODEL.

Let us consider a PV array affected by shading. At any instant, we can state:

$$P_S = P_{NS} \cdot \left(1 - F_{ES}\right) \tag{2}$$

where P_S and P_{NS} represent the power delivered by the PV array with and without shading respectively, and F_{ES} so-called here as effective shading factor, whose value determines the power decrease.

A first possible F_{ES} estimation consists on assuming that the power reduction is just equal to shaded array fraction. This is the geometrical shading factor F_{GS}:

$$F_{ES} = F_{GS} \tag{3}$$

In fact, this approximation represents a minimum limit for power reduction. Hence, it is always optimistic[ref].

A second approximation, this time pessimistic[ref], is to assume that any shadow fully cancels power:

$$F_{GS} > 0 \quad \Rightarrow \quad F_{ES} = 1 \tag{4}$$

A better approximation is obtained by taking into account the shaded blocks. A “block” is here defined as a group of cells protected by one bypass diode. A block is shaded when at least one of its cells is shaded. A first possibility is to consider that the power of a block is fully cancelled when the block is shaded. Hence:

$$(1 - F_{ES}) = \left(1 - \frac{N_{SB}}{N_{TB}}\right) \tag{5}$$

where N_{TB} is the total number of blocks inside the concerned array and N_{SB} is the number of shaded blocks. This approximation tends to be optimistic.

A more accurate approximation is to use the following expression, which takes into account both the shaded fraction of the array area and the number of blocks affected by shade.

$$(1 - F_{ES}) = (1 - F_{GS}) \cdot \left(1 - \frac{N_{SB}}{N_{TB} + 1}\right) \tag{6}$$

The number “1” added in the denominator has not direct physical sense: it is a mathematical trick to avoid fully cancel power when a shadow affects all the array blocks (N_{SB} = N_{TB}) but still keeps a significant illuminated area (low F_{GS}). It is worth stressing that equation (6) is purely experimental and its physical interpretation may lack of sense. For example, for a large value of N_{TB} the ratio N_{SB} / (N_{TB} + 1) tends toward F_{GS}. Hence (1-F_{ES}) ≈ (1-F_{GS})^2. Another example: when all blocks are shaded (N_{SB} = N_{TB}) the ratio N_{SB} / (N_{TB} + 1) varies between 0·5 (N_{TB} = 1) and 1 (N_{TB} >> 1), which is unreal because it implies that the power losses caused by the same shadow repeated on several PV modules increase as the number of PV modules increases. Actually, the power losses could be equal (imagine a parallel connection of all the PV modules) and they depends on the particular reverse characteristics of solar cells[ref]. Obviously, the simplicity of the proposed model does not allow taking into consideration such electrical characteristics of the PV array, which would require the simulation of the I-V curve. In return, and despite its limitations, the model performs relatively well, which has been checked in the experimental testing campaign present below.

In practical terms, F_{ES} must only be applied to the directional components of the in-plane irradiance: direct, B, and circumsolar part of diffuse, D^{CIR}. Neither isotropic diffuse, D^{ISO}, nor albedo, R, are significantly affected by shading. Hence:

$$P_S = P^* \cdot \left[1 + \gamma \cdot \left(T_C - T_C^*\right)\right] \cdot \frac{\left[\left(B + D^C\right) \cdot \left(1 - F_{ES}\right) + D^I + R\right]}{G^*} \qquad (7)$$

This expression can also be written in terms of power decrease:

$$\left(1 - \frac{P_S}{P_{NS}}\right) = \left(1 - \frac{\left[\left(B + D^{CIR}\right) \cdot \left(1 - F_{ES}\right) + D^{ISO} + R\right]}{G}\right) \qquad (8)$$

3. EXPERIMENTAL VERIFICATION.

Several experiments consisting of measuring the I-V curves of real PV arrays (array A, array B and array C) both with and without shading have been carried out.

Then, we have compared the experimental power reduction with the calculated one in accordance with equation (7), where the F_{ES} value is estimated as presented in equation (3), equation (4) or equation (5).

3.1. Array A.

Figure 1 shows some of the “ad-hoc” shading profiles cast over array A: a 376 W PV array installed at the IES-UPM terrace.

Figure 1. Examples of shading profiles cast over array A

Figure 2a shows the internal constitution of the PV modules involved: they are made up of 33 solar cells connected in series and two bypass diodes which have overlapping cells, i.e., each diode is between 22 solar cells and both diodes protect the eleven central solar cells. So, array A has N_{TB} = 16 blocks. The eight modules in array A have been arranged in three configurations (Figure 2b): one string of eight modules (left); two strings of four modules (middle); and four strings of two modules (right). It is worth noting that, for a given shadow size and shape, N_{SB} is the same regardless of the electrical configuration of the PV array (Figure 2c).

Figure 2. a) Internal connection of cells and bypass diodes inside modules of array A. b) Configurations of array A: one string of 8 modules (left); two strings of 4 modules (middle); and four strings of 2 modules (right). c) Two particular examples of shadows cast over array A (Figure 1b and Figure 1c respectively).

As an example, Figure 3 shows the I-V curves corresponding to a particular configuration (Figure 2b middle) and two particular shades (just, Figure 1b and Figure 1c, also represented in Figure 2c). Table 1 presents the experimental power reduction resulting from the impact of the shadow and the estimated one through equation (8) by using different values of F_{ES}, calculated in accordance with equation (3), equation (4), equation (5) or equation (6). Clearly, equation (6) leads to a much better estimation than equation (3), equation (4) and equation (5).

Figure 3. Current - Voltage (I-V, left graphic) and Power – Voltage (P-V, right one) curves of Array A made up of two strings of 4 modules (configuration Figure 2b middle) corresponding to shading profiles of Figure 1b (triangles) and Figure 1c (crosses). Circles represent the curve without the impact of the shadow.

Table 1. Power measurement of array A (connected as Figure 2b middle), related to the particular shadows presented in Figure 2c, characterised by F_{GS} and N_{SB}. Experimental power reduction is shown in column "Exp". Model power reductions estimated with equation (8) and in accordance with equation (3), equation (4), equation (5) and equation (6) are also presented. The individual estimation error is in brackets and italics.

Table 2 and Figure 4 present the results of extending the experiment to a vast number of shading situations on array A connected as in Figure 2b middle. In Table 2, F_{GS} is defined as the product of the geometrical shadow factor horizontal, $F_{GS,H}$, and the geometrical shadow factor vertical, $F_{GS,V}$. Again, the model proposed here (equation (8) with F_{ES} in accordance with equation (6)) leads to Mean Error and Root Mean Square Error (ME and RMSE respectively) values significantly lower than equation (3), equation (4) and equation (5), and it behaves reasonably well for all the shade range.

Table 2. Experimental ("Exp") and estimated ("Eq 3", "Eq 4", "Eq 5" and "Eq 6") power reduction of array A connected as Figure 2b middle. These values are related to the set of shades characterised by F_{GS} and N_{SB}. F_{GS} is defined as the product of horizontal and vertical geometrical shadow factor, $F_{GS,H}$ and $F_{GS,V}$. The individual estimation error is in brackets and italics. The Mean Error and Room Mean Square Error are also presented.

Figure 4. Model power reduction estimated with equation (8) versus experimental power reduction for the set of shading profiles cast over array A, connected as Figure 2b middle. Discontinuous line points out agreement between estimation and experimental values. Triangles, crosses, squares and circles represent, respectively, the estimation of power reduction related to F_{ES} calculated in accordance with equation (3), equation (4), equation (5) and equation (6).

Along the same lines, Table 3 summarizes the results for the same shading profiles cast over array A, but now arranged in the other configurations (figure 2b left and right). Again, equation (6) leads to ME and RMSE significantly lower than equation (3), equation (4) and equation (5).

Table 3. The Mean Error and Room Mean Square Error of estimated power reduction of array A, connected as Figure 2b left and right. Values for approximations in accordance with equation (3), equation (4), equation (5) and equation (6) are presented.

3.2. Array B.

Figure 5a shows the internal constitution of the PV modules of array B: they are made up of 48 solar cells connected in series and three bypass diodes. Each diode protects 16 solar cells. So, array B has N_{TB} = 12 blocks. The four modules of array B have been arranged in three configurations (Figure 5b): one string of four modules (left); two strings of two modules (middle); and four strings of one module (right).

Another “ad-hoc” set of shading profiles, similar to the one used on array A, has been cast over array B. Table 4 presents the ME and RMSE related to the three configurations. Again, equation (6) leads to results much better than equation (3), equation (4) and equation (5).

Figure 5. a) Internal connection of cells and bypass diodes inside modules of array B. b) Configurations of array B: one string of 4 modules (left); two strings of 2 modules (middle); and four strings of 1 module (right).

Table 4. Mean Error and Room Mean Square Error of estimated power reduction of array B, for all the configurations shown in Figure 5b. Values for approximations in accordance with equation (3), equation (4), equation (5) and equation (6) are presented.

3.3. Array C.

Finally, the experimental campaign has been extended to commercial PV plants. Figure 6 shows the case of a 1 MW PV plant located near Almería (Spain), with 40 PV arrays. Each 25 kW PV array is made up of 160 PV modules, and each module comprises 2 bypass diodes.

Figure 6. Shading profiles cast over 25 kW PV arrays of a commercial PV plant installed in Almería (Spain).

One of these arrays, array C, has been measured. Figure 7 presents the agreement between experimental and estimated power reduction and Table 5 summarizes these results. Again, equation (6) performs remarkably better than the others.

Table 5. Mean Error and Room Mean Square Error of estimated power reduction of array C. Values for approximations in accordance with equation (3), equation (4), equation (5) and equation (6) are presented.

Figure 7. Model power reduction estimated with Equation (8) versus experimental power reduction for the set of shading profiles cast over array C. The discontinuous line highlights the agreement between the estimation and experimental values. Triangles, crosses, squares and circles represent, respectively, the estimation of power reduction

related to F_{ES} calculated in accordance with equation(3), equation (4), equation (5) and equation (6).

3.4. Energy yield simulation and shading losses.

Individual large error estimations presented previously can surprise the reader. However, it has to be taken into account that the final goal is to estimate the energy yield. As a representative example, the case of a 2 axis tracking PV plant at Madrid has been calculated. The 2 axis trackers have been designed in accordance with the dynamic symmetry of root rectangles[ref]: PV module size 1x√2 m^2, PV tracker with 18 modules 6x3√2 m^2 and ground tracker distribution 10.4x10.4√2 m^2 (NSxEW distances between tracker axes). So the ground cover ratio is GCR = 1/6. The selected PV modules is characterised by having 3 diodes, i.e., 3 blocks, in such a way that 3x18 blocks (vertical x horizontal) can be identified at each tracker. By using IES-UPM's own code, described elsewhere[ref], the energy yield has been simulated. Shading losses associated with equation (3), equation (4), equation (5) and equation (6) have been 2.1, 11.3, 2,7 and 3.9 % respectively. Experimental losses in real PV systems with similar GCR are about 5 %[ref].

4. CONCLUSIONS.

A simple mathematical model for the estimation of PV array power reduction resulting from shading has been presented. A key advantage of this model is that it can be applied to direct power calculations, i.e., without the need to solve the full I-V curve. A wide experimental testing campaign has demonstrated the good performance of this model.

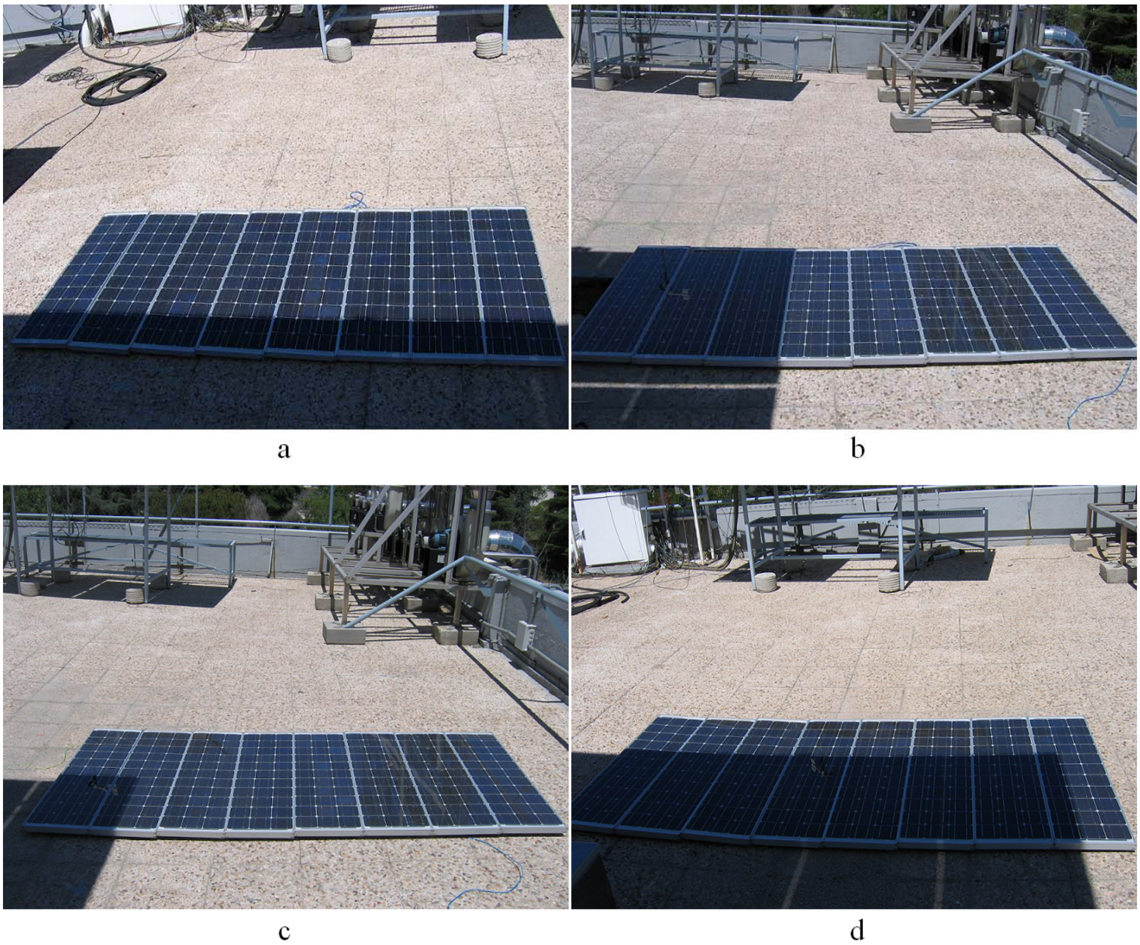

Figure 1. Examples of shading profiles cast over array A.

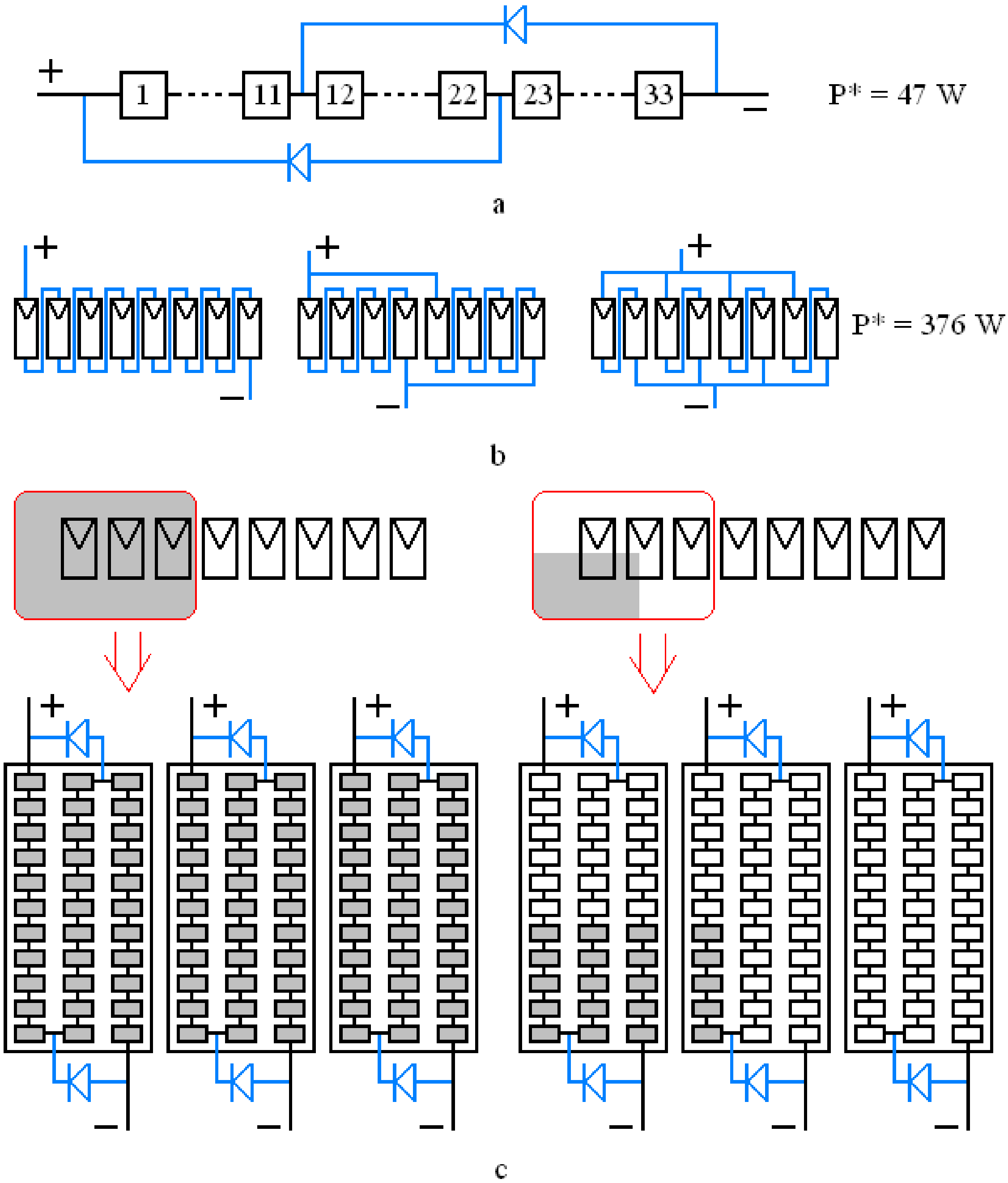

Figure 2. a) Internal connection of cells and bypass diodes inside modules of array A. b) Configurations of array A: one string of 8 modules (left); two strings of 4 modules (middle); and four strings of 2 modules (right). c) Two particular examples of shadows cast over array A (Figure 1b and Figure 1c respectively).

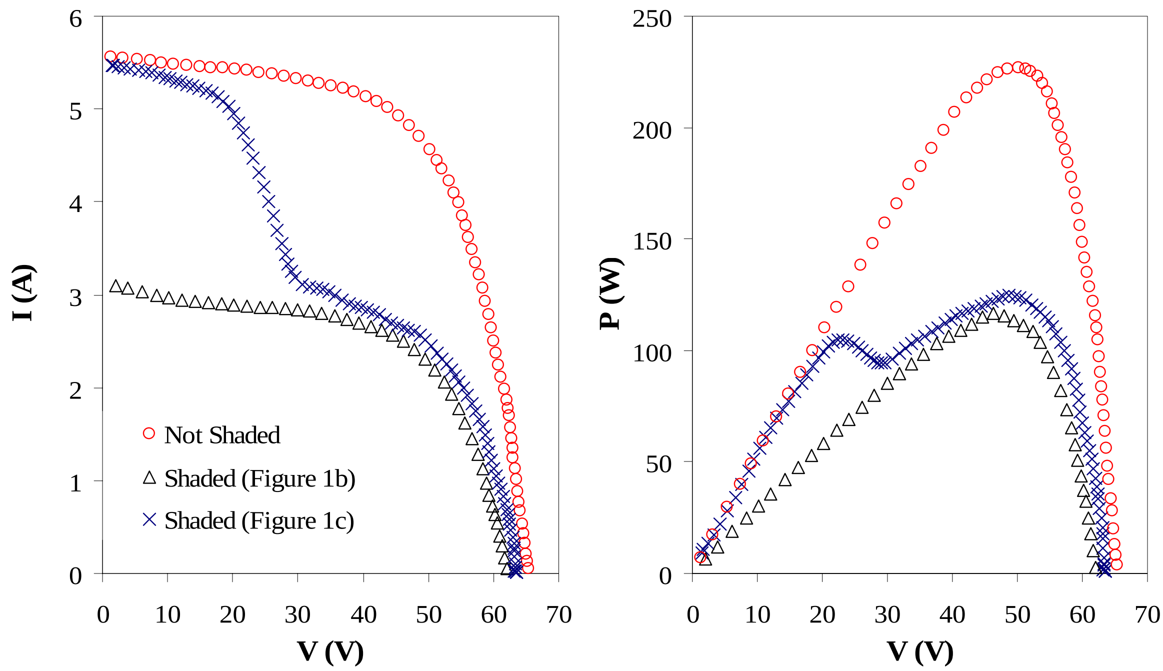

Figure 3. Current - Voltage (I-V, left graphic) and Power – Voltage (P-V, right one) curves of Array A made up of two strings of 4 modules (configuration Figure 2b middle) corresponding to shading profiles of Figure 1b (triangles) and Figure 1c (crosses). Circles represent the curve without the impact of the shadow.

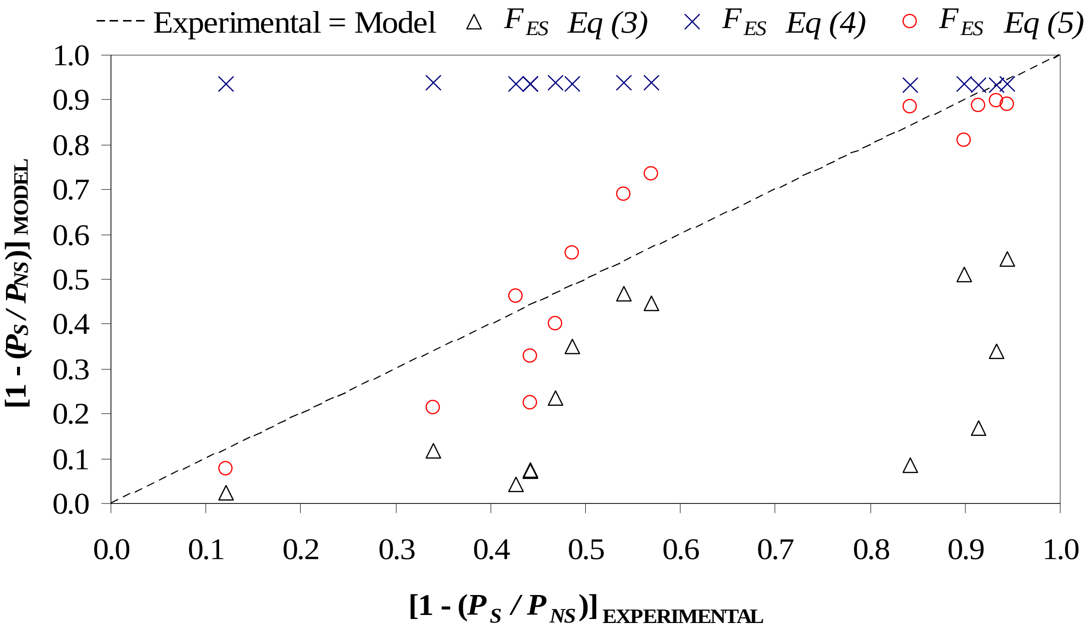

Figure 4. Model power reduction estimated with equation (8) versus experimental power reduction for the set of shading profiles cast over array A, connected as Figure 2b middle. Discontinuous line points out agreement between estimation and experimental values. Triangles, crosses, squares and circles represent, respectively, the estimation of power reduction related to F_{ES} calculated in accordance with equation (3), equation (4), equation (5) and equation (6).

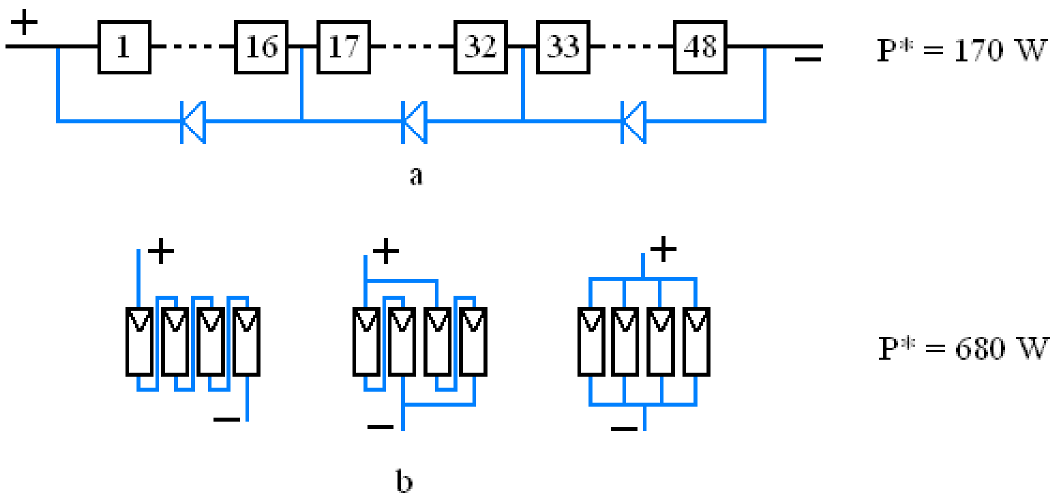

Figure 5. a) Internal connection of cells and bypass diodes inside modules of array B. b) Configurations of array B: one string of 4 modules (left); two strings of 2 modules (middle); and four strings of 1 module (right).

Figure 6. Shading profiles cast over 25 kW PV arrays of a commercial PV plant installed in Almería (Spain).

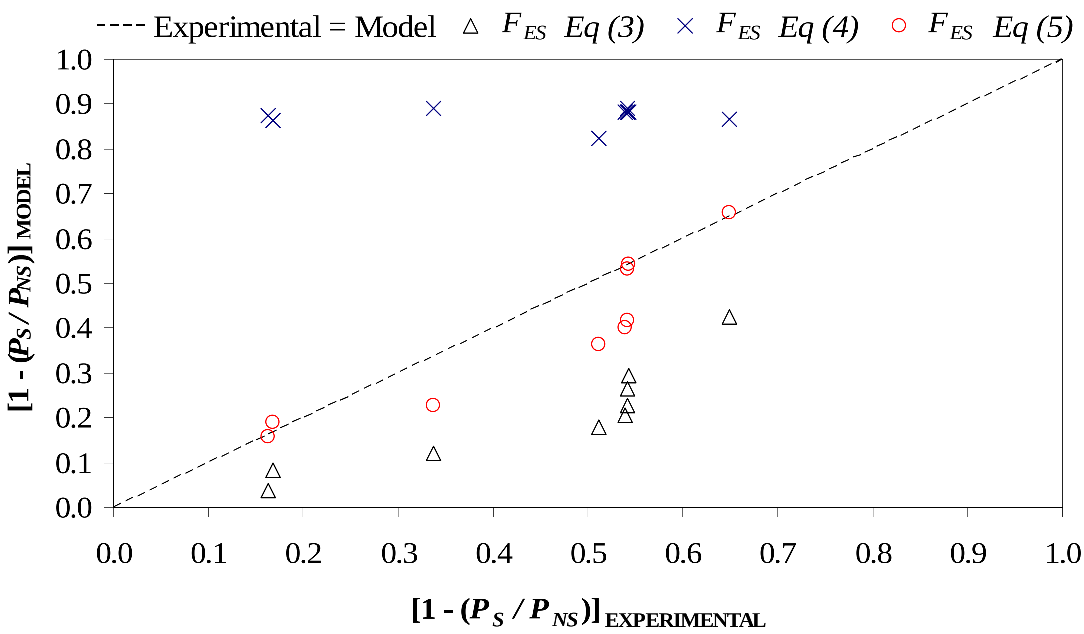

Figure 7. Model power reduction estimated with Equation (8) versus experimental power reduction for the set of shading profiles cast over array C. The discontinuous line highlights the agreement between the estimation and experimental values. Triangles, crosses, squares and circles represent, respectively, the estimation of power reduction related to F_{ES} *calculated in accordance with equation(3), equation (4), equation (5) and equation (6).*

Shadow	F_{GS} **(%)**	N_{SB} **(%)**	P_S **(W)**	P_{NS} **(W)**	**(P_{NS} - P_S) / P_{NS}** *(Eq (X) – Exp)/Exp (%)*				
					Exp	**Eq (3)**	**Eq (4)**	**Eq (5)**	**Eq (6)**
Figure 1 b (Figure 2c left)	7.6	6	116.5	226.8	0.49	0.35 *(-28 %)*	0.94 *(92 %)*	0.35 *(-28 %)*	0.56 *(15 %)*
Figure 1 c (Figure 2c right)	37.5	3	124.6	223.2	0.44	0.07 *(-84 %)*	0.94 *(112 %)*	0.18 *(-60 %)*	0.22 *(-49 %)*

Table 1. Power measurement of array A (connected as Figure 2b middle), related to the particular shadows presented in Figure 2c, characterised by F_{GS} and N_{SB}. Experimental power reduction is shown in column "Exp". Model power reductions estimated with equation (8) and in accordance with equation (3), equation (4), equation (5) and equation (6) are also presented. The individual estimation error is in brackets and italics.

SHADOW	$F_{GS,H}$	$F_{GS,V}$	N_{SB}	$(P_{NS} - P_S) / P_{NS}$ *(Eq (X) - Exp) / Exp (%)*				
				EXP	**Eq (3)**	**Eq (4)**	**Eq (5)**	**Eq (6)**
	1,00	0,09	16	0,84	0,08 *(-90)*	0,93 *(11)*	0,93 *(11)*	0,88 *(5)*
	1,00	0,18	16	0,91	0,17 *(-81)*	0,93 *(2)*	0,93 *(2)*	0,89 *(-3)*
	1,00	0,36	16	0,93	0,34 *(-64)*	0,93 *(0)*	0,93 *(0)*	0,90 *(-4)*
	0,04	0,64	1	0,12	0,02 *(-80)*	0,93 *(670)*	0,06 *(-52)*	0,08 *(-35)*
	0,17	0,45	3	0,44	0,07 *(-84)*	0,94 *(112)*	0,18 *(-60)*	0,22 *(-49)*
	0,29	0,27	5	0,44	0,07 *(-83)*	0,94 *(112)*	0,29 *(-34)*	0,33 *(-26)*
	0,50	0,09	8	0,43	0,04 *(-90)*	0,94 *(119)*	0,47 *(10)*	0,46 *(9)*
	0,13	1,00	2	0,34	0,12 *(-66)*	0,94 *(176)*	0,12 *(-66)*	0,21 *(-37)*
	0,25	1,00	4	0,47	0,23 *(-50)*	0,94 *(100)*	0,23 *(-50)*	0,40 *(-15)*
	0,38	1,00	6	0,49	0,35 *(-28)*	0,94 *(92)*	0,35 *(-28)*	0,56 *(15)*
	0,50	1,00	8	0,54	0,47 *(-13)*	0,94 *(74)*	0,47 *(-13)*	0,69 *(28)*
	0,58	0,82	10	0,57	0,45 *(-21)*	0,94 *(65)*	0,59 *(3)*	0,74 *(29)*
	0,75	0,73	12	0,90	0,51 *(-43)*	0,94 *(4)*	0,70 *(-22)*	0,81 *(-10)*
	0,92	0,64	15	0,94	0,55 *(-42)*	0,94 *(-1)*	0,88 *(-7)*	0,89 *(-6)*
				ME (%)	*-60*	*110*	*-22*	*-7*
				RMSE	*27*	*171*	*27*	*24*

Table 2. Experimental ("Exp") and estimated ("Eq 3", "Eq 4", "Eq 5" and "Eq 6") power reduction of array A connected as Figure 2b middle. These values are related to the set of shades characterised by F_{GS} and N_{SB}. F_{GS} is defined as the product of horizontal and vertical geometrical shadow factor, $F_{GS,H}$ and $F_{GS,V}$. The individual estimation error is in brackets and italics. The Mean Error and Room Mean Square Error are also presented.

	Configuration Figure 2b left				Configuration Figure 2b right			
	Eq (3)	**Eq (4)**	**Eq (5)**	**Eq (6)**	**Eq (3)**	**Eq (4)**	**Eq (5)**	**Eq (6)**
ME (%)	-63	115	-28	-14	-55	120	-17	1
RMSE	20	205	20	12	29	124	23	25

Table 3. The Mean Error and Room Mean Square Error of estimated power reduction of array A, connected as Figure 2b left and right. Values for approximations in accordance with equation (3), equation (4), equation (5) and equation (6) are presented.

		ME (%)	RMSE
Configuration Figure 5b left	**Eq (3)**	-56	23
	Eq (4)	84	113
	Eq (5)	-25	23
	Eq (6)	-9	18
Configuration Figure 5b left	**Eq (3)**	-47	26
	Eq (4)	154	238
	Eq (5)	-15	9
	Eq (6)	8	23
Configuration Figure 5b right	**Eq (3)**	-48	27
	Eq (4)	-115	120
	Eq (5)	-15	20
	Eq (6)	6	26

Table 4. Mean Error and Room Mean Square Error of estimated power reduction of array B, for all the configurations shown in Figure 5b. Values for approximations in accordance with equation (3), equation (4), equation (5) and equation (6) are presented.

	Eq (3)	Eq (4)	Eq (5)	Eq (6)
ME (%)	-56	152	-41	-11
RSME	12	160	15	16

Table 5. Mean Error and Room Mean Square Error of estimated power reduction of array C. Values for approximations in accordance with equation (3), equation (4), equation (5) and equation (6) are presented.